nature medicine

Crosstalk between B lymphocytes, microbiota and the intestinal epithelium governs immunity versus metabolism in the gut

Natalia Shulzhenko[1,10,11], Andrey Morgun[1,10,11], William Hsiao[2], Michele Battle[3], Michael Yao[4], Oksana Gavrilova[5], Marlene Orandle[6], Lloyd Mayer[7], Andrew J Macpherson[8], Kathy D McCoy[8,9], Claire Fraser-Liggett[2] & Polly Matzinger[1]

Using a systems biology approach, we discovered and dissected a three-way interaction between the immune system, the intestinal epithelium and the microbiota. We found that, in the absence of B cells, or of IgA, and in the presence of the microbiota, the intestinal epithelium launches its own protective mechanisms, upregulating interferon-inducible immune response pathways and simultaneously repressing Gata4-related metabolic functions. This shift in intestinal function leads to lipid malabsorption and decreased deposition of body fat. Network analysis revealed the presence of two interconnected epithelial-cell gene networks, one governing lipid metabolism and another regulating immunity, that were inversely expressed. Gene expression patterns in gut biopsies from individuals with common variable immunodeficiency or with HIV infection and intestinal malabsorption were very similar to those of the B cell–deficient mice, providing a possible explanation for a longstanding enigmatic association between immunodeficiency and defective lipid absorption in humans.

The mammalian gut is a complex ecosystem with three main interacting components: the intestinal epithelium with its neuronal connections, the gut-associated immune tissue and the commensal microbiota. These components have several bidirectional interactions. The microbiota, for example, are essential for the emergence of T cell subsets and the differentiation of gut B cells into IgA-producing plasma cells[1–7]. Conversely, hosts that lack T and B cells, that make only IgM antibodies or that have defective innate immune sensors show changes in intestinal microbiota[8–10] that sometimes lead to metabolic abnormalities and obesity[8]. Between the commensals and the intestinal epithelium, some dialogues induce the epithelium to produce specific fucosylated glycans[11,12], whereas others increase energy harvest from food[13].

It has been proposed that trialogues may also govern gut metabolism[14], but there has been no direct evidence for this idea. Here we show that a trialogue does indeed exist. A defect in adaptive immunity indirectly influences the balance between metabolic and immune functions of the gut epithelium via a three-way conversation between the two host systems and the intestinal microbiota.

Normally, immune protection in the gut results from a partnership between the immune system (supplying B cells, T cells and innate immune cells) and the epithelium (supplying antimicrobial peptides and a mucosal layer that hinders bacterial invasion[2,15]). To begin deciphering the immune system's effect on the homeostatic functions of the gut epithelium, we studied global gene expression in the jejunum of B cell–deficient mice. In the presence of the microbiota, the intestinal epithelium in these mice launched its own defense mechanisms, activating innate immune genes at the expense of metabolic ones primarily regulated by the transcription factor Gata4. This created a defect in fat absorption resulting in decreased body fat and leptin levels. The molecular features of the malabsorption found in the B cell–deficient mice were also present in IgA-deficient mice, humans with common variable immunodeficiency (CVID) and humans with HIV infection.

These data support our previous suggestion that tissues take an active role in their own defense[16,17]. When the immune system functions optimally, the intestinal epithelium can concentrate on its metabolic functions. However, if the immune system is dysfunctional, the epithelium takes on some of the missing immune functions at the expense of its metabolic activity. This is also the first example, to our knowledge, of a trialogue (in mice and humans) in which the adaptive immune system, the intestine and the microbiota govern a homeostatic metabolic function.

[1]'Ghost Lab', T Cell Tolerance and Memory Section, Laboratory of Cellular and Molecular Immunology, National Institute of Allergy and Infectious Diseases (NIAID), US National Institutes of Health (NIH), Bethesda, Maryland, USA. [2]Institute for Genome Sciences, University of Maryland School of Medicine, Baltimore, Maryland, USA. [3]Department of Cell Biology, Neurobiology & Anatomy, Medical College of Wisconsin, Milwaukee, Wisconsin, USA. [4]Mucosal Immunology Section, Laboratory of Host Defenses, NIAID, NIH, Bethesda, Maryland, USA. [5]Mouse Metabolism Core Laboratory, National Institute of Diabetes and Digestive and Kidney Diseases, NIH, Bethesda, Maryland, USA. [6]Comparative Medicine Branch, NIAID, NIH, Bethesda, Maryland, USA. [7]Immunology Institute, Mount Sinai Medical Center, New York, New York, USA. [8]University of Bern, Bern, Switzerland. [9]Farncombe Family Digestive Health Research Institute, McMaster University, Hamilton, Ontario, Canada. [10]Present address: College of Pharmacy, Oregon State University, Corvallis, Oregon, USA. [11]These authors contributed equally to this work. Correspondence should be addressed to A.M. (anemorgun@hotmail.com), N.S. (natalia.shulzhenko@oregonstate.edu) or P.M. (pcm@helix.nih.gov).

Received 19 April; accepted 9 September; published online 20 November 2011; doi:10.1038/nm.2505

RESULTS

Gene expression in the gut of B cell–deficient mice

B cells are among the most prominent populations of immune cells in the small intestine's lamina propria, presumably because of their role in protection from pathogens. We started studying their role in intestinal homeostasis by examining gene expression in the jejunum of B cell–deficient (BcKO) mice. To exclude effects of particular mutations or of unique background genes, we included mice carrying two different mutations preventing B cell development (μMT: carrying a deletion in the transmembrane domain of the IgM heavy chain; and JhKO: carrying a deletion in the J segment of the immunoglobulin heavy chain locus) on two different strain backgrounds (B10.A and BALB/c). To identify robust gene profiles, we used large sample sizes (27 mice per group, see **Supplementary Fig. 1a**) and compared homozygous deficient mice to heterozygous littermates and also to wild-type (WT) non-littermates (**Fig. 1a**). After we excluded genes expressed in B cells, about 280 genes (298 gene-probes) showed expression differences between both types of BcKO mice and their respective controls (**Fig. 1b**, **Supplementary Table 1** and **Supplementary Fig. 1b**). Here we refer to this set of genes as the 'BcKO profile'.

By Gene Ontology enrichment analysis, most of the genes upregulated in B cell–deficient intestines were involved in immunity, including genes related to defense, inflammatory and interferon-inducible responses (**Fig. 1c** and **Supplementary Fig. 2a**). These results suggest that loss of one part of the immune system (B cells) leads to compensatory changes in other parts.

The downregulated genes were mostly involved in various metabolic processes (**Fig. 1d**), predominantly oxidation and reduction (electron transport, energy generation) and lipid, steroid and cholesterol metabolism and transport. These changes were not due to simple loss of intestinal epithelium, as careful morphological examination showed no differences between BcKO and control mice (**Supplementary Fig. 2b**). This downregulation of metabolism-related gene programs suggests that the intestinal epithelium, despite normal morphology, cannot optimally handle nutrients or perform metabolic functions in the absence of B cells.

IgA is crucial for normal intestinal gene expression

Although B cells might affect gut homeostasis in several ways[18,19], the most likely is via antibody production. We therefore studied the gene expression profile of AID and μS double–knockout mice, which carry a deletion in the gene for activation-induced cytidine deaminase, and a deletion in the secretion-specific portion of the gene encoding IgM. These mice have B cells but do not produce secreted antibodies[9,20]. The correlation ($r = 0.8$) between the 280-gene profile of the antibody-deficient and of the two types of BcKO mice (**Fig. 2a**) was nearly as good as the correlation ($r = 0.85$) between the two BcKO strains themselves (**Fig. 2b**), showing that antibody deficiency accounts for most of the gene expression properties of the B cell–deficient phenotype.

Because IgA is the major antibody class in the gut, we next obtained the intestinal expression profiles of mice deficient for IgA by virtue of a deletion in *Igh-2* (IgAKO). The comparison of gene expression alterations in BcKO and IgAKO mice (to their respective controls) indicated that about 70% of the phenotype seen in BcKO mice seemed to be due to the absence of IgA (**Fig. 2c**), despite a ~100-fold compensatory increase in intestinal IgM gene expression (**Fig. 2d**). Thus, the majority of the intestinal effects of B cells seem to be mediated by IgA, and only a few depend on other B cell functions.

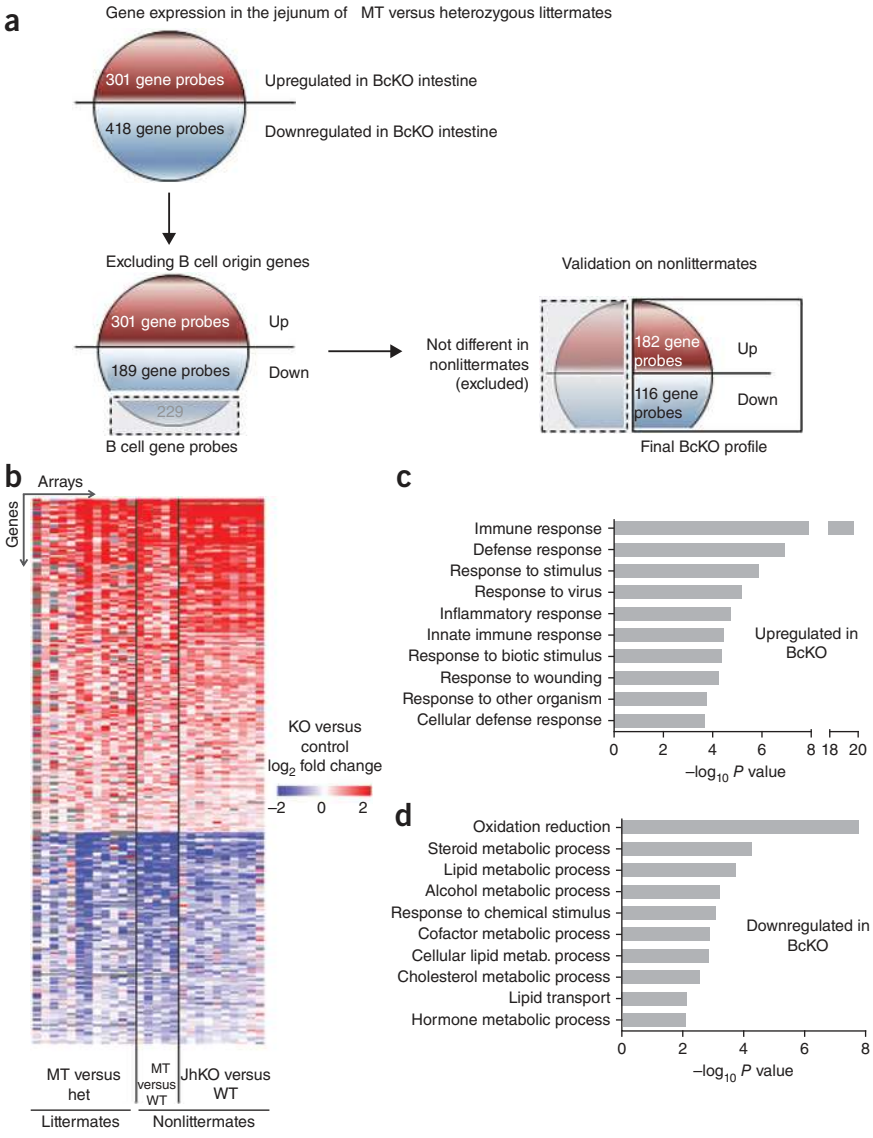

Figure 1 Dysregulation of gene expression in the small intestine of BcKO mice. (**a**) Diagram of the discovery of the BcKO profile (see details in Methods). (**b**) Heatmap of the differentially expressed genes (BcKO profile) in the jejunum of BcKO mice and their corresponding controls (false discovery rate <10%). Each line represents one gene probe; each column represents one array; color represents the difference between BcKO and the corresponding control on that array, blue indicating lower and red higher expression in BcKO mice; gray color indicates missing values; het, heterozygous. (**c**,**d**) Enrichment of Gene Ontology categories (Biological Process) for the up- (**c**) and downregulated (**d**) genes in BcKO mice. The top ten categories are shown.

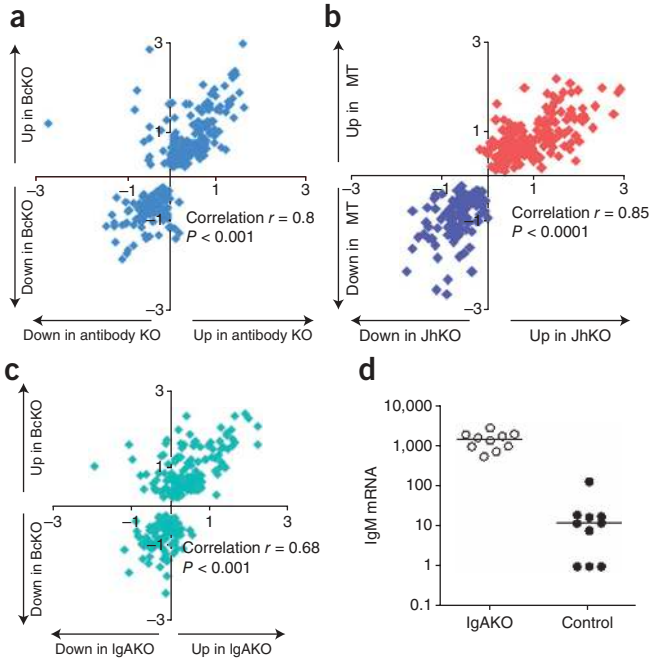

Figure 2 Dysregulation of gene expression is present in the gut of antibody-deficient and IgA-deficient mice. (**a**) Gene expression ratios between BcKO and control (WT and heterozygous) mice (*y* axis, $n = 27$ per group) and between antibody-deficient versus heterozygous control mice (*x* axis; $n = 9$ per group). (**b**) Gene expression ratios in two strains of BcKO mice: B10A-μMT versus control (WT and heterozygous) mice (*y* axis, $n = 17$ per group) and BALB/c-JhKO versus WT control mice (*x* axis; $n = 10$ per group). (**c**) Gene expression ratios between BcKO and control (*y* axis; 27 per group) and between immunoglobulin A-deficient (IgA) and heterozygous control (*x* axis; $n = 10$ per group) mice. Similarity of gene expression profile between the experiments was estimated using Pearson's correlation. Each symbol represents one gene from the BcKO profile established in **Figure 1**. The values on axes are $\log_2$ fold change knockout versus control. (**d**) Levels of IgM transcripts (probe intensities on arrays) in the jejunum of IgA KO and heterozygous control mice ($P < 0.001$).

Microbiota are essential for the B cell effect

Because most of the antibodies in the gut are directed against the microbiota[21], a plausible scenario would be that IgA deficiency leads to general overgrowth of microbes and/or greater microbial access to the jejunum of BcKO mice. We found no difference in total amounts of bacterial DNA (**Fig. 3a**), but serum lipopolysaccharide (LPS) concentrations were higher in BcKO mice compared to control mice (**Supplementary Fig. 2c**), suggesting that antibody deficiency might change the species distribution within the microbial community. We therefore analyzed the microbiota in the jejunum by sequencing DNA coding for 16S bacterial ribosomal RNA (a highly conserved gene) and comparing the compositions of different taxa. To control for non–genotype-related factors (such as age, environment and parentage) we performed pairwise comparisons of sex-matched BcKO and control littermates. To control for potential seasonal changes in parameters such as lighting, and for different batches of food and bedding, we did two independent experiments 4 months apart. Overall, the bacterial composition was similar among control and BcKO mice (**Supplementary Fig. 3a**). However, there were moderate differences in three families. BcKO mice harbored fewer Clostridiacea-family bacteria and more of the *Paracoccus* genus (Rhodobacteraceae family) and of a specific operational taxonomic unit (OTU) comprising the *Lactococcus* genus subgroup F49WGKH02HS7CN (Streptococcaceae family; **Supplementary Data**) (**Fig. 3b**). All these bacteria were minority representatives of the community in both BcKO and control mice, with the most abundant one (Clostridiacea) making up only about 0.4% of the jejunal bacteria (**Supplementary Fig. 3b**), suggesting that small changes within the microbial community may promote substantial alterations in intestinal function. Alternatively, these changes in bacterial populations may be a side effect of antibody deficiency and have little role in the metabolic changes we saw.

To test these possibilities, we derived germ-free lines of BcKO mice (both μMT and JhKO), plus their corresponding germ-free controls, and compared their jejunal gene expression profiles. The expression differences between BcKO and WT mice disappeared under germ-free conditions for all but six genes of the BcKO profile (**Fig. 3c**). All of the germ-free mice, regardless of their B cell status, resembled the conventionally reared WT controls (**Fig. 3d**) rather than the conventionally reared BcKO mice, suggesting that the microbiota do indeed have a role in the decline of metabolic gut function that occurs in the absence of B cells.

We next asked whether the phenotype required precisely the microbial populations of the BcKO mice or whether any microbes would do. We did a four-way comparison by colonizing germ-free BcKO and heterozygous control littermates with microbiota from BcKO or heterozygous control mice. After ~3 weeks, the gene expression changes of these colonized mice were governed by their genotypes rather than by the source of colonizing microbiota (**Fig. 3e**,**f** and **Supplementary Fig. 4a**). For example, the expression ratios between conventionally raised BcKO and control mice versus those of the germ-free–reconstituted mice were similar, whether the reconstituting microbiota came from control (**Fig. 3e**) or BcKO (**Fig. 3f**) mice. Thus, microbial interactions are necessary for the expression of the BcKO phenotype, but the host's genotype governs the final outcome.

Gata4-related metabolic defects in BcKO mice

To determine how B cells and the microbiota regulate intestinal metabolism, we searched the promoters of the downregulated genes in the BcKO profile for any highly represented transcription factor binding sites. There were almost seven times more Gata4-binding sites among these promoters than among promoters of ~1,000 jejunally expressed genes that did not differ between BcKO and controls or among promoters of all known mouse genes (**Fig. 4a**). Gata4 is a key player in intestinal gene regulation and function, where it is specifically expressed in epithelial cells[22,23].

To ask how genes in the BcKO profile might behave in the presence of B cells but the absence of Gata4, we studied mice that specifically lack Gata4 expression only in the intestinal epithelium (Gata4KO^{vil}) by virtue of a deletion in the *Gata4* gene generated by Cre recombinase expressed under a villin promoter[23]. Approximately 60% of the gene expression changes in BcKO mice were also present in Gata4KO^{vil} mice (**Fig. 4b** and **Supplementary Table 2**), indicating that the majority of the gene expression changes in the BcKO mice were due to impaired Gata4-dependent functions. These changes were specific to Gata4, as deletions in two other intestinally active transcription factors (Ppara and Klf9)[24,25] did not lead to similar changes (**Supplementary Fig. 4b**).

Several genes that were concordantly regulated in Gata4KO^{vil} and BcKO mice are involved in fat uptake and metabolism. *Slc27a2* encodes a fatty acid transporter[26]; *Osbpl3* encodes an intracellular lipid receptor[27]; and *Acaa1b*, *Clps*, *Agmo* and *Apoc3* encode proteins involved in lipid oxidation, hydroxylation or catabolism. Mice lacking *Pdk4* are resistant to the diabetogenic effects of high-fat diets[28–30], and Gata4KO^{vil} mice have impaired fat and, especially,

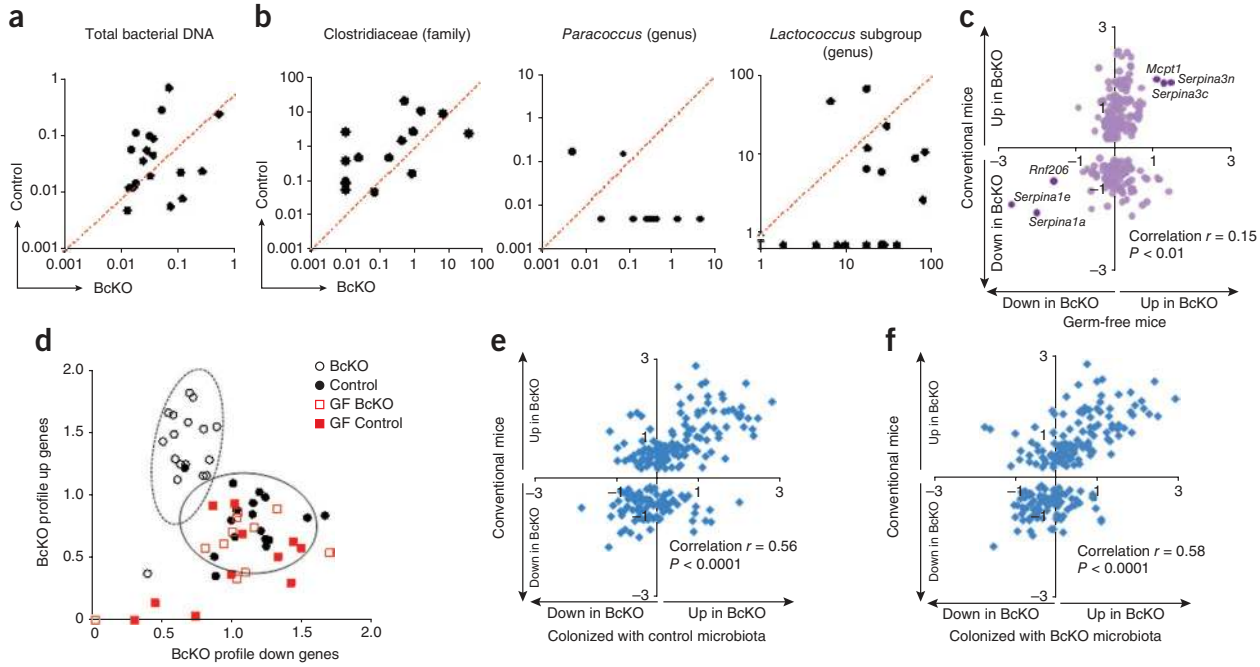

Figure 3 Microbiota are necessary for intestinal alterations in BcKO mice. (**a**) Amount of total bacterial DNA (ng) per 10 ng of isolated total DNA from jejunum content of BcKO and control mice (each dot represents data from two mice of the same litter). (**b**) Amount of DNA (pg) for Clostridiacea (family), *Paraccococus* (genus) and for an operational taxonomic unit corresponding to a subgroup of *Lactococcus* (genus) per 10 ng of isolated total DNA from jejunum content of BcKO and control mice. Data represented as in **a**. (**c**) Gene expression ratios between BcKO and control (WT and heterozygous) (*y* axis; $n = 27$ per group) and between germ-free BcKO versus germ-free control (WT and heterozygous) mice (*x* axis; $n = 11$ per group). Six genes that are differentially expressed between germ-free BcKO and germ-free control mice are labeled. (**d**) Two-dimensional visualization of the gene expression of upregulated (BcKO profile up) and downregulated (BcKO profile down) genes in four groups of mice. Each symbol represents one mouse. Values are summary metrics of upregulated (*y* axis) and downregulated (*x* axis) genes of the BcKO profile. Ellipses represent two s.d. from the centroids for BcKO (dashed line) and Control (solid line) groups. GF, germ-free. (**e**) Gene expression ratios between conventional BcKO and control (WT and heterozygous) mice (*y* axis; $n = 27$ per group) and between ex–germ-free BcKO versus control mice colonized with microbiota from control mice (*x* axis; $n = 8$ per group). (**f**) Gene expression ratios between conventional BcKO and control (WT and heterozygous) mice (*y* axis; $n = 27$ per group) and between ex–germ-free BcKO versus control mice colonized with microbiota from control mice (*x* axis; $n = 5$ per group). Each symbol in **c**,**e**,**f** represents one gene from the BcKO profile, and the values on axes are $\log_2$ fold change for knockout versus control.

cholesterol absorption[23]. We therefore examined lipid uptake in the BcKO mice and found that their cholesterol and fat absorption were indeed less efficient compared to the corresponding heterozygous littermates (**Fig. 4c** and **Supplementary Fig. 5a**), though there was no difference in overall food intake (**Supplementary Fig. 5b**). We also compared the amounts of fat carried by homozygous BcKO

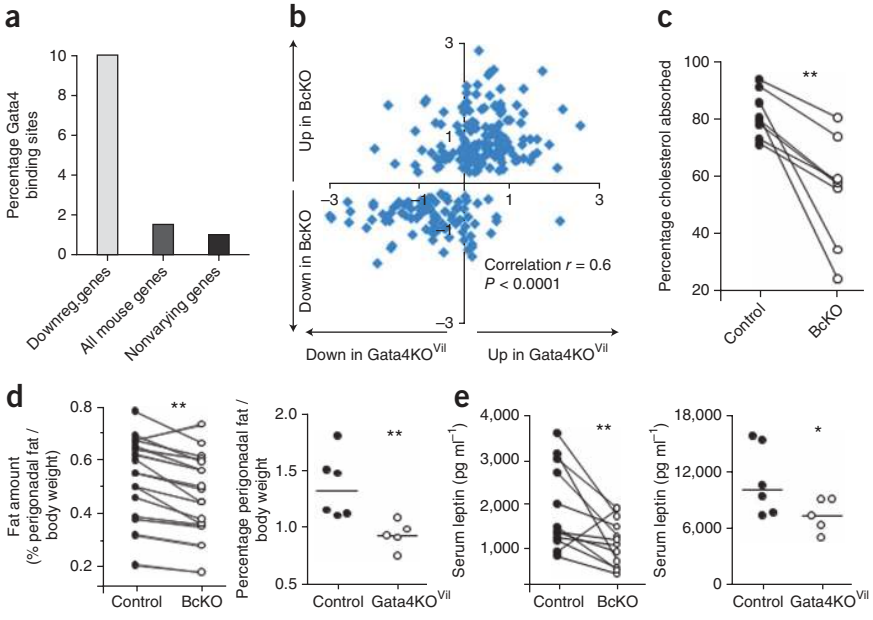

Figure 4 Dysregulation of Gata4-dependent functions in BcKO mice. (**a**) Proportion of Gata4 binding sites in the promoters of downregulated genes from BcKO profile, promoters of all known mouse genes and of ~1,000 nonvarying genes expressed in the jejunum ($P < 1 \times 10^{-14}$). (**b**) Gene expression ratios ($\log_2$) between BcKO versus WT and heterozygous control (*y* axis; $n = 27$ per group) and between Gata4KO^{vil} versus heterozygous control mice (*x* axis; $n = 5$ per group). Each symbol represents one gene. (**c**) Intestinal cholesterol absorption in BcKO and heterozygous littermates. Each dot represents one mouse. Each line represents one litter. (**d**) Proportion of perigonaldal fat (grams) in relation to total body weight (grams) in BcKO (left), Gata4KO^{vil} (right) and their corresponding heterozygous control mice. (**e**) Serum leptin levels in BcKO (left) and Gata4KO^{vil} (right) mice and their corresponding heterozygous control mice. (*$P < 0.05$; **$P < 0.01$). In **d**,**e**, for BcKO and control mice, each dot represents median value of each genotype in a given litter and each line represents one litter. For Gata4KO^{vil} mice, each dot represents one mouse.

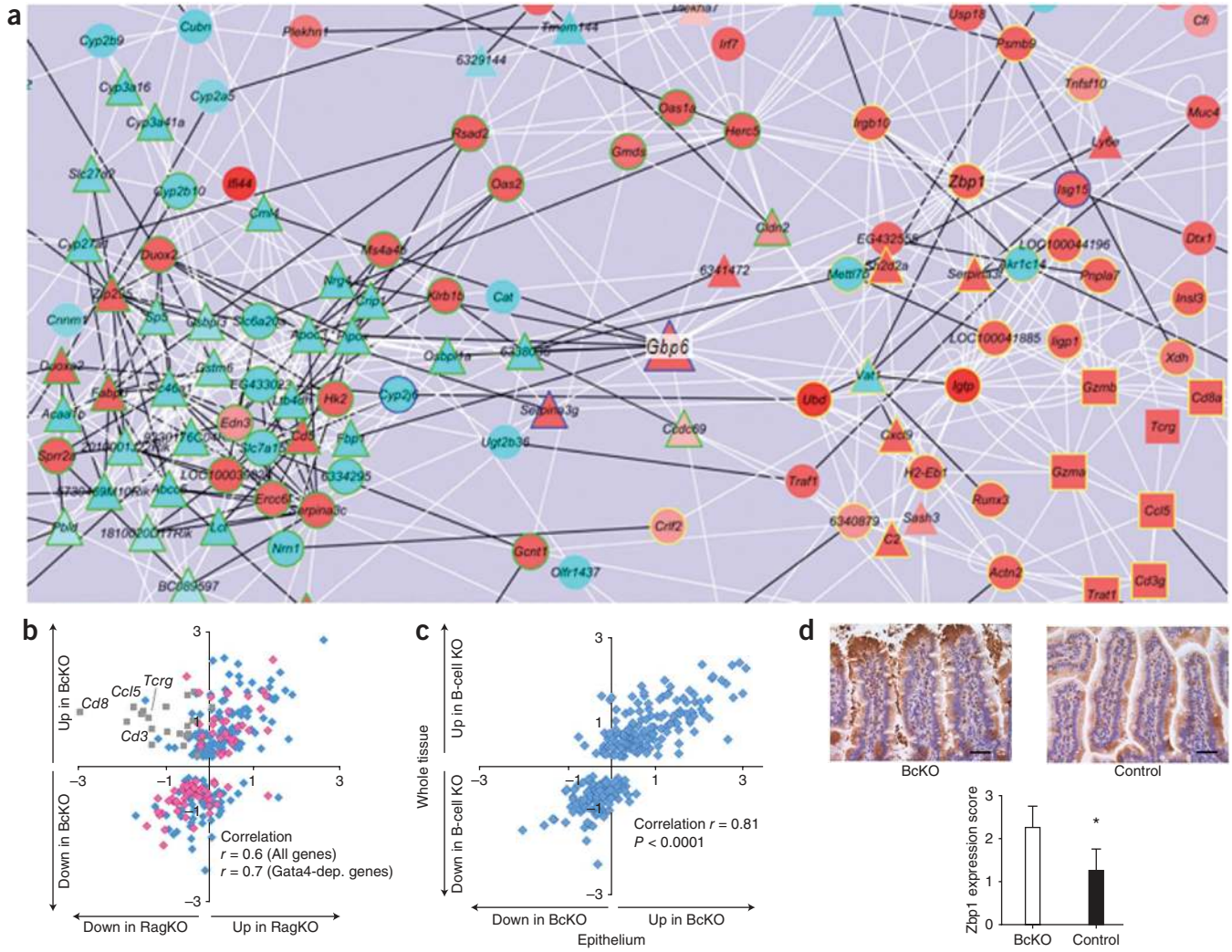

Figure 5 Increased immune and decreased metabolic state of epithelium in BcKO mice. (**a**) Gene expression network of BcKO profile reconstructed from the data of control mice (zoomed in to the central part of the network; the whole network is in **Supplementary Fig. 5a**). Each line represents a correlation, and each node represents a gene. White lines are positive and black are negative correlations; triangles are Gata4-dependent genes, squares are the T cell genes and circles are all other genes; red node fills indicate upregulation, and light blue fills are downregulation; green node outline is a subnetwork 1, yellow is a subnetwork 2, blue is both subnetworks, and unoutlined node symbols do not belong to either of the two subnetworks. (**b**) Gene expression ratios ($\log_2$) between BcKO versus control (*y* axis; $n = 27$ per group) and between RAG2-knockout (RagKO) versus control (*x* axis; $n = 8$ per group) mice. Each symbol represents one gene. Grey squares are T cell–related genes. Pink diamonds are Gata4-dependent genes; blue are all other genes. (**c**) Gene expression ratios ($\log_2$) between gut whole tissue of BcKO versus control mice (*y* axis; $n = 27$ per group) and between intestinal epithelium of BcKO versus control mice (*x* axis; $n = 3$ per group). Each symbol represents one gene. (**d**) Immunohistochemistry for Zbp1 in jejunum of BcKO and control mice (left) and the results of semiquantitative blind evaluation (right; $n = 4$, $^*P < 0.05$; bars represent s.d.); scale bars, 40 μm.

versus heterozygous B cell–sufficient littermates on both regular and high-fat diets and by Gata4KO^{vil} versus control mice. Both types of deficient mice had significantly lower amounts of perigonadal fat than their controls, regardless of diet (**Fig. 4d** and **Supplementary Fig. 5c**). We also assessed other body fat stores (inguinal, mesenteric) and general adiposity by nuclear magnetic resonance in an independent group of BcKO mice and found decreased amounts of fat compared to heterozygous littermate controls (**Supplementary Fig. 5e**). Finally, because fat stores correlate with systemic leptin levels[31], we measured serum leptin concentrations in Gata4KO^{vil} and BcKO mice and found lower amounts of leptin in both types of deficient mice than in controls (**Fig. 4e** and **Supplementary Fig. 5d**,**e**). Thus, many of the metabolic changes seen in BcKO mice seem to be Gata4 dependent.

Immune and metabolic gene networks in gut epithelium

The BcKO profile consists of two parts that are not obviously related: downregulated metabolic and upregulated immune genes (**Fig. 1c**). To search for a physiological link between them, we used a recently developed analytical tool for reconstruction of gene expression networks[32]. Correlations in expression of the genes in the BcKO profile in a group of 39 normal mice (comprising both WT and heterozygous mice) revealed a network of 228 interconnected genes containing 688 connections and two major subnetworks (**Fig. 5a** and **Supplementary Fig. 6a**). The first subnetwork (77 genes, 56% downregulated), incorporated many of the downregulated metabolic genes, two-thirds of which were Gata4 dependent, and was highly enriched for genes governing lipid transport and other metabolic processes (**Supplementary Fig. 6b**). The second subnetwork (41 genes, 88%

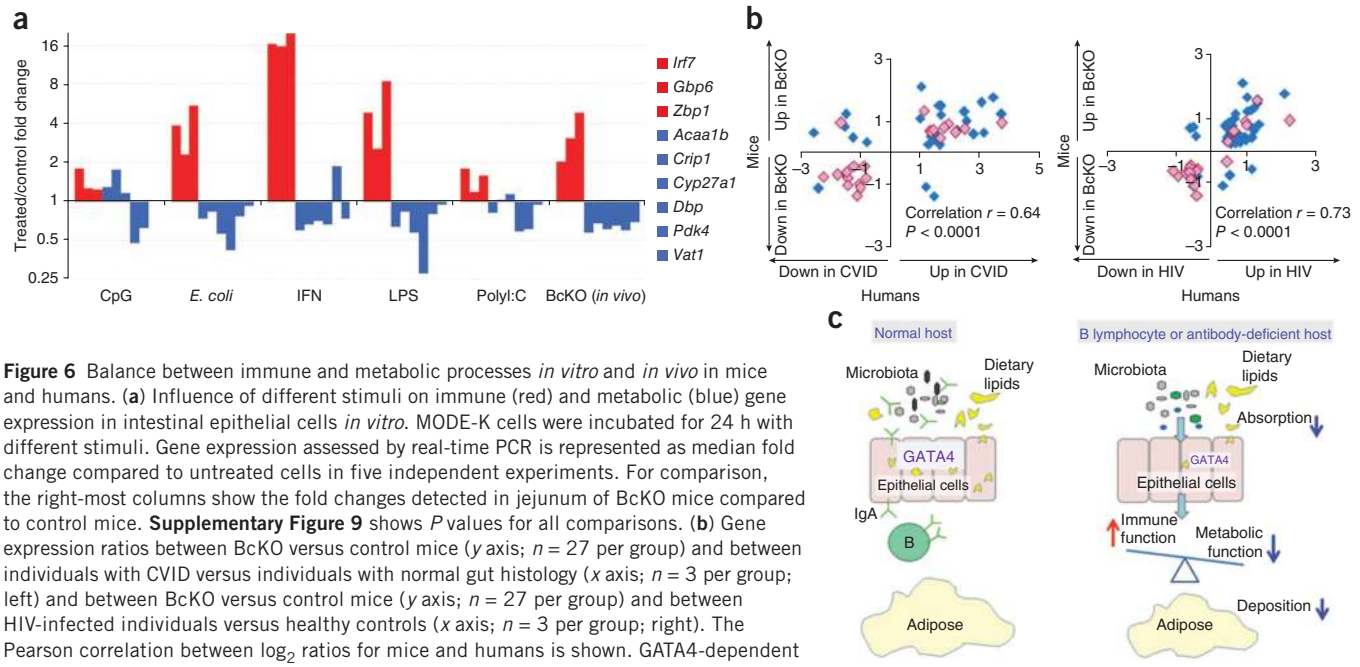

Figure 6 Balance between immune and metabolic processes *in vitro* and *in vivo* in mice and humans. (**a**) Influence of different stimuli on immune (red) and metabolic (blue) gene expression in intestinal epithelial cells *in vitro*. MODE-K cells were incubated for 24 h with different stimuli. Gene expression assessed by real-time PCR is represented as median fold change compared to untreated cells in five independent experiments. For comparison, the right-most columns show the fold changes detected in jejunum of BcKO mice compared to control mice. **Supplementary Figure 9** shows *P* values for all comparisons. (**b**) Gene expression ratios between BcKO versus control mice (*y* axis; $n = 27$ per group) and between individuals with CVID versus individuals with normal gut histology (*x* axis; $n = 3$ per group; left) and between BcKO versus control mice (*y* axis; $n = 27$ per group) and between HIV-infected individuals versus healthy controls (*x* axis; $n = 3$ per group; right). The Pearson correlation between $\log_2$ ratios for mice and humans is shown. GATA4-dependent genes are shown in pink. (**c**) A schematic diagram illustrating that, unlike the situation with replete B cells, the balance between immune and metabolic processes within gut epithelial cells in hosts lacking B lymphocytes or IgA antibodies is skewed towards an immune response against microbiota (gray, black, green and blue ovoid objects) at the expense of GATA4-related metabolism, mainly lipid absorption and deposition.

upregulated) contained mostly upregulated immune and inflammatory genes (**Supplementary Fig. 6c**).

These metabolic and immune subnetworks are connected by five genes and are inversely regulated (**Fig. 5a**). This might reflect the activity of two interacting cell types (for example, epithelial and immune cells) or of two sets of genes within a single cell (for example, metabolic and immune genes in epithelium). We found an indication for the first scenario that pointed to T cells, as the immune subnetwork contains a minigroup of highly connected T cell–specific genes (*Cd3g*, *Gzma*, *Gzmb*, *Cd8a*, *Tcrg* and *Ccl5*; **Fig. 5a**), and flow cytometry analysis revealed an increased proportion of $CD8^+$ and $CD4^+CD8^+$ T cells in the jejunum of BcKO mice (**Supplementary Fig. 7**), consistent with an earlier report that μMT BcKO mice harbor elevated populations of highly cytotoxic intestinal $CD8^+$ T lymphocytes[33]. Downmodulation of intestinal metabolic functions might thus be due to the negative effects of over-exuberant T cell cytotoxic responses. To test this possibility, we analyzed the BcKO profile in RAG2-knockout mice (which lack both B and T cells) and found that the lack of T cells had little impact on the BcKO profile (except for T cell–related genes) and even less effect on Gata4-dependent genes (**Fig. 5b**).

The alternative scenario, that there might be a molecular switch between immune and metabolic processes within the epithelial cells themselves, was suggested by our finding that a single gene (*Gbp6*, encoding an interferon-inducible GTPase[34]) strongly connects the two subnetworks and correlates positively with immune and negatively with metabolic subnetwork genes. To test this hypothesis, we isolated intestinal epithelial cells (with <5% intraepithelial T cells) and compared their expression of the BcKO profile with that of the intact whole tissue. The epithelium-specific expression profile resembled that of the whole tissue (**Fig. 5c**), with a correlation ($r = 0.81$) similar to that between the two types of BcKO mice ($r = 0.85$, **Fig. 2b**). Protein amounts (of a small number of testable genes) followed the mRNA levels. On western blots, interferon-induced GTPase abundance was elevated in BcKO epithelial cells compared to heterozygous controls, whereas the metabolic proteins acetyl-CoA acyltransferase 1 and lactase were suppressed (**Supplementary Fig. 8**). Histologically, expression of Zbp1 (Z DNA binding protein, a cytosolic bacterial DNA sensor and activator of interferon (IFN)-regulatory factors[35]), one of the most connected genes in the immune subnetwork, was also elevated in epithelium of BcKO versus heterozygous control mice (**Fig. 5d**). Altogether, these data suggest that changes in the intestinal epithelial cells themselves are primarily responsible for the immune and metabolic phenotype we see in the whole-tissue analysis.

Microbe effects on epithelium

Because the epithelial differences between BcKO and control mice were evident only when microbes were present, we asked whether the microbes act directly on the epithelium or indirectly by activating immune cells that, in turn, affect epithelial function. To test this, we added *Escherichia coli* and Toll-like receptor ligands to the mouse epithelial cell line MODE-K and measured the expression of Gata4-dependent metabolic genes. Although most intestinal epithelial cell lines stop expressing many metabolic genes that are expressed *in vivo*, we found that the MODE-K cell line retains expression of a few of the Gata4-related metabolic genes in the BcKO profile. Treating MODE-K cells with heat-inactivated *E. coli*, or with LPS, decreased the expression of most of the metabolic genes and simultaneously induced expression of immune genes (**Fig. 6a**). Poly I:C had an effect on half of the tested genes, and CpG treatment induced no significant changes in most of the genes (**Fig. 6a**). To test the prediction from the network analysis that IFN-dependent responses would downregulate metabolic genes, we also added a combination of IFN-α and IFN-γ and found that this did indeed cause a direct inhibition of metabolic function (**Fig. 6a** and **Supplementary Fig. 9**). Therefore, in the absence of B cells or of IgA, the intestinal epithelium itself responds to microbes, upregulating IFN-inducible immune response pathways and simultaneously repressing Gata4-related metabolic functions.

Immunodeficiencies in humans

Several features led us to the hypothesis that our results linking B cells, intestinal epithelium and microbiota might be relevant to humans. First, the intestinal microbiota are crucial in host energy uptake and fat metabolism and have been linked to human obesity (reviewed in ref. 36). Second, the *GATA4* gene is ~90% conserved between humans and mice, with similar tissue mRNA expression levels (**Supplementary Fig. 10**). Third, two human immunodeficiencies (CVID and secondary immunodeficiency caused by HIV infection) have similar gastrointestinal syndromes with unexplained malabsorption, low weight gain and steatorrhea (fatty stools)[37–41]. Although the CVID syndrome was first described ~60 years ago[42], the molecular pathogenesis of the intestinal defects in either immunodeficiency is still unclear[43,44].

To determine whether the molecular mechanisms found in the BcKO mice might also operate in the human disease, we analyzed gene expression profiles of duodenal biopsies from three humans with CVID with gastrointestinal pathology and three immunodeficient subjects with normal duodenal histology. For HIV, we used recently published gene expression data comparing HIV-infected individuals to healthy uninfected people[45]. The gene expression differences between immunodeficient humans and their respective controls were remarkably similar to the results from BcKO mice (**Fig. 6b**). Genes concordantly upregulated in immunodeficient mice and humans largely involved immune components, such as T cell genes (*CD8A*, *CD5*, *TNFSF10*), interferon-induced genes (*RSAD2*, *OAS2*, *IFI44*, *IFITM*, *HLA-C*, *HLA-DRB1*) and complement (**Supplementary Tables 3** and **4**), whereas the downregulated profile contained mostly metabolic functions such as lipid and carbohydrate metabolism (*APOC3*, *PDK4*, *HPGD*, *FBP1*), oxidative reduction (*IYD*) and transport of micronutrients, including vitamins (*ABCC6*, *SLC46A1*, *OPLAH*). Finally, ~95% of the Gata4-dependent genes were concordantly regulated in both the BcKO mice and the human immunodeficiencies (**Fig. 6b**), suggesting that these genes are directly involved in the human malabsorption and impaired lipid deposition (**Fig. 6c**).

DISCUSSION

Our data uncover a three-way conversation in the small intestine between the epithelium, B cells and the microbiota that moderates immunity and also influences intestinal and systemic metabolic homeostasis. This trialogue affects the balance between immune IFN-related and metabolic GATA4-related functions within epithelial cells in both humans and mice, and it seems to be involved in the previously unexplained malabsorption and consequent malnutrition in people with primary and secondary immunodeficiency (from CVID and HIV, respectively).

Although B cells have several functions in immunity[18,19,46,47], we found that their effect on intestinal metabolism depends on their ability to secrete IgA (the antibody normally found in mucosal surfaces). Most intestinal IgA is directed against intestinal flora[2], and it can have several different effects. It restricts bacterial access to the epithelium and to intestinal immune cells[2,48], and it can change the molecules expressed by bacteria[49] or promote survival of specific bacteria[50]. To isolate the relevant IgA function, we analyzed the microbiota found in normal and B cell–deficient mice. The total numbers of luminal bacteria were similar, and there was no obvious pathogen among the bacteria in BcKO mice. Rather, there were changes in three minor commensal bacterial subsets. This left us with three possibilities. First, the BcKO phenotype was unrelated to the microbiota. Second, minor changes in the microbiota were sufficient to cause the phenotype. Or, third, changes in the activity, rather than the diversity of the intestinal microbiota, were important. To test the first, we derived germ-free B cell–deficient and littermate control mice and found that the BcKO phenotype did indeed depend on the microbiota. To test the second, we transferred the microbiota from BcKO and control mice to germ-free mice and found that both populations of microbes induced the B cell–deficient phenotype in BcKO germ-free recipients, whereas neither induced the phenotype in WT germ-free mice. Together, these results suggested that microbes were needed to reveal the B cell–deficient phenotype, but no particular microbe was essential. However, in a preliminary study, we found that colonization with pure *Lactobacillus reuteri* (one of the most common jejunal bacteria in both BcKO and heterozygous control mice) did not induce the phenotype (data not shown), suggesting that contact with a particular microbe, or an interacting group of microbes, may be important. The higher levels of serum LPS that we found in BcKO mice suggest that the microbes in these mice are in greater contact with the gut tissue, perhaps directly signaling the epithelium to the presence of the offending bacteria. These results support the idea that disease does not necessarily require the presence of a 'classical' pathogen. Commensals may cause disease or not, depending on the host's genotype, as the functional activity of the same microbe might differ depending on the host[49].

Because the absence of B cells resulted in the increased expression of many immune genes, we asked whether the downregulation of metabolic function in epithelial cells was an indirect result of increased activity by cells of the immune system or a result of changes of expression in the epithelium itself. By network analysis, we found that the epithelial cells have two interacting gene networks, one governing lipid metabolism (mostly regulated by Gata4) and one governing innate immunity (mostly made up of IFN-dependent genes) that are inversely connected via a small number of genes, with the main one being *Gbp6*, an IFN-inducible gene suggested to have antibacterial function[34]. Isolated epithelial cells from BcKO mice, tested immediately *ex vivo*, showed increased immune function and decreased metabolic function at both the RNA and protein levels. Further, an epithelial cell line responded directly to bacteria and bacterial components, as well as to IFNs, by upregulating immune genes and downregulating metabolic ones. Together, these data suggest that the intestinal epithelium responds to bacteria, and to inflammatory signals, by upregulating its own immune functions while downregulating its metabolic ones. The reverse can also occur, as we saw that the intestinal cells of Gata4KO^{vil} mice, which have decreased metabolic function and gene expression, have simultaneously increased their expression of immune genes.

It is noteworthy that the connections between the epithelial immune and metabolic functions are not specific to B cell deficiency, as the gene expression network was reconstructed on the basis of the variability of gene expression seen in normal mice. Therefore, the interplay between immune and metabolic processes within epithelial cells is a normal physiological process that becomes skewed in the small intestine of mice lacking B cells.

Immunodeficient humans with CVID or HIV have several features in common with the BcKO and IgAKO mice, suggesting that the underlying mechanism of the gastrointestinal disorders is similar in the two species. First, as in BcKO mice, no pathogen has consistently been associated with gastrointestinal syndrome in people with CVID or HIV[38,43]. Second, in some cases, HIV-infected people have low populations of intestinal IgA-secreting plasma cells[43,51,52]. Third, although many immunodeficient humans are routinely treated with IgG infusions (which help to protect them from infections),

such infusions do not ameliorate the gastrointestinal problems in CVID[38,44]. Similarly, two months of IgG injections did not result in any normalization of the intestinal gene expression profile of BcKO mice (data not shown). Our finding that IgA is the major B cell product maintaining the metabolic trialogue suggests that it might be useful to develop a pool of stable, intestinal IgA molecules to add to the current treatment protocol. Fourth, there is a link through GATA4. The expression of GATA4-dependent genes is similarly affected in BcKO mice and in CVID and HIV intestinal biopsies, suggesting that the molecular mechanism of malabsorption is similar in mice and humans. It has been proposed that these metabolic alterations might result from harmful activity of cytotoxic T cells residing in the gut of immunodeficient people[38]. Our results, however, indicate that T cells have little influence on the metabolic dysbalance; rather, epithelial cells themselves redirect their activity from metabolic to immune function in response to changes in the microenvironment. Therefore, treatment for GI syndrome might need to be refocused from generic anti-inflammatory medication to specific modulation of GATA4-dependent activity of epithelial cells.

Finally, our study supports our previous proposal[16,17] that tissues take an active role in their own immune protection. In the presence of a functional adaptive immune system, the intestinal epithelium can concentrate on its metabolic functions. However, if the adaptive immune system is dysfunctional (in this case because it lacks B cells), the intestinal epithelium takes on some of the missing immune functions at the expense of its metabolic activity (**Fig. 6c**). It will be worthwhile to investigate further how often such diversion is the basis for autoimmune disease.

METHODS

Methods and any associated references are available in the online version of the paper at http://www.nature.com/naturemedicine/.

Accession codes. Gene expression files containing array data are available under the GSE23934 superseries in the Gene Expression Omnibus (GEO) data repository. All microbiome data are deposited in the National Center for Biotechnology Information (NCBI) Sequence Read Archive under accession number SRP003253.

Note: Supplementary information is available on the Nature Medicine website.

ACKNOWLEDGMENTS

This research was supported in part by the Intramural Research Program of the NIAID, NIH. We thank T. Myers, Q. Su and A. Godinez of the NIAID microarray facility for excellent technical support; R. Schwartz for providing funding for germ-free re-derivation; W. Strober for help with human subjects; C. Jones for technical support of bacterial pyrosequencing; T.D. Randall (Trudeau Institute) for AID/μS mice; S. Epstein (US Food and Drug Administration), J. Misplon (US Food and Drug Administration) and D.P. Huston (Texas A&M Health Science Center) for IgAKO mice; D. Kaiserlian (Institut National de la Santé et de la Recherche Médicale) and R. Blumberg (Harvard University) for providing the MODE-K cell line; R. Varma for help in experiments; Laboratory of Cellular and Molecular Immunology members and M. Sterman Dolnikoff, I. Shmulevich and A. Dzutsev for discussions and suggestions; Y. Kotliarov for help with graphics; S. Varma for help finding human gene homologues; J. Coursen for excellent technical support; B. Epstein for assistance with software programming; and the personnel of NIH mouse facilities in buildings 4 and 6B. The Cincinnati Mouse Metabolic Phenotyping Center is supported by NIH grant U24 DK059630 and National Gnotobiotic Rodent Resource Center at the University of North Carolina is supported by grant P40RR018603.

AUTHOR CONTRIBUTIONS

N.S. and A.M. conceived the original idea, designed the study, conducted most of the experiments, analyzed the data and wrote the manuscript. W.H. analyzed microbiome data and drafted the related part of the manuscript. M.B. provided Gata4KO^{vil} mice and did some Gata4-related experiments. M.Y. and L.M. collected duodenal biopsies and performed clinical evaluation of human subjects. O.G. performed and analyzed experiments related to lipid metabolism. M.O. performed histological evaluation of mouse samples. A.J.M. and K.D.M. re-derived germ-free JhKO mice and collected organs. C.F.-L. supervised microbiome evaluation and drafted the related part of the manuscript. P.M. supervised the whole study and wrote the manuscript.

COMPETING FINANCIAL INTERESTS

The authors declare no competing financial interests.

Published online at http://www.nature.com/naturemedicine/.
Reprints and permissions information is available online at http://www.nature.com/reprints/index.html.

1. Cerf-Bensussan, N. & Gaboriau-Routhiau, V. The immune system and the gut microbiota: friends or foes? *Nat. Rev. Immunol.* **10**, 735–744 (2010).
2. Hooper, L.V. & Macpherson, A.J. Immune adaptations that maintain homeostasis with the intestinal microbiota. *Nat. Rev. Immunol.* **10**, 159–169 (2010).
3. Umesaki, Y., Setoyama, H., Matsumoto, S., Imaoka, A. & Itoh, K. Differential roles of segmented filamentous bacteria and clostridia in development of the intestinal immune system. *Infect. Immun.* **67**, 3504–3511 (1999).
4. Ivanov, I.I. *et al.* Induction of intestinal T_H17 cells by segmented filamentous bacteria. *Cell* **139**, 485–498 (2009).
5. Gaboriau-Routhiau, V. *et al.* The key role of segmented filamentous bacteria in the coordinated maturation of gut helper T cell responses. *Immunity* **31**, 677–689 (2009).
6. Klaasen, H.L. *et al.* Apathogenic, intestinal, segmented, filamentous bacteria stimulate the mucosal immune system of mice. *Infect. Immun.* **61**, 303–306 (1993).
7. Round, J.L. & Mazmanian, S.K. Inducible Foxp3$^+$ regulatory T-cell development by a commensal bacterium of the intestinal microbiota. *Proc. Natl. Acad. Sci. USA* **107**, 12204–12209 (2010).
8. Vijay-Kumar, M. *et al.* Metabolic syndrome and altered gut microbiota in mice lacking Toll-like receptor 5. *Science* **328**, 228–231 (2010).
9. Fagarasan, S. *et al.* Critical roles of activation-induced cytidine deaminase in the homeostasis of gut flora. *Science* **298**, 1424–1427 (2002).
10. Suzuki, K. *et al.* Aberrant expansion of segmented filamentous bacteria in IgA-deficient gut. *Proc. Natl. Acad. Sci. USA* **101**, 1981–1986 (2004).
11. Umesaki, Y., Okada, Y., Matsumoto, S., Imaoka, A. & Setoyama, H. Segmented filamentous bacteria are indigenous intestinal bacteria that activate intraepithelial lymphocytes and induce MHC class II molecules and fucosyl asialo GM1 glycolipids on the small intestinal epithelial cells in the ex-germ-free mouse. *Microbiol. Immunol.* **39**, 555–562 (1995).
12. Bry, L., Falk, P.G., Midtvedt, T. & Gordon, J.I. A model of host-microbial interactions in an open mammalian ecosystem. *Science* **273**, 1380–1383 (1996).
13. Turnbaugh, P.J. *et al.* An obesity-associated gut microbiome with increased capacity for energy harvest. *Nature* **444**, 1027–1031 (2006).
14. Gordon, J.I., Hooper, L.V., McNevin, M.S., Wong, M. & Bry, L. Epithelial cell growth and differentiation. III. Promoting diversity in the intestine: conversations between the microflora, epithelium, and diffuse GALT. *Am. J. Physiol.* **273**, G565–G570 (1997).
15. Treiner, E. *et al.* Selection of evolutionarily conserved mucosal-associated invariant T cells by MR1. *Nature* **422**, 164–169 (2003).
16. Matzinger, P. Tolerance, danger and the extended family. *Annu. Rev. Immunol.* **12**, 991–1045 (1994).
17. Matzinger, P. & Kamala, T. Tissue-based class control: the other side of tolerance. *Nat. Rev. Immunol.* **11**, 221–230 (2011).
18. Mizoguchi, A., Mizoguchi, E., Takedatsu, H., Blumberg, R.S. & Bhan, A.K. Chronic intestinal inflammatory condition generates IL-10–producing regulatory B cell subset characterized by CD1d upregulation. *Immunity* **16**, 219–230 (2002).
19. Golovkina, T.V., Shlomchik, M., Hannum, L. & Chervonsky, A. Organogenic role of B lymphocytes in mucosal immunity. *Science* **286**, 1965–1968 (1999).
20. Carragher, D.M., Kaminski, D.A., Moquin, A., Hartson, L. & Randall, T.D. A novel role for non-neutralizing antibodies against nucleoprotein in facilitating resistance to influenza virus. *J. Immunol.* **181**, 4168–4176 (2008).
21. Macpherson, A.J. *et al.* A primitive T cell–independent mechanism of intestinal mucosal IgA responses to commensal bacteria. *Science* **288**, 2222–2226 (2000).
22. Bosse, T. *et al.* Gata4 is essential for the maintenance of jejunal-ileal identities in the adult mouse small intestine. *Mol. Cell. Biol.* **26**, 9060–9070 (2006).
23. Battle, M.A. *et al.* GATA4 is essential for jejunal function in mice. *Gastroenterology* **135**, 1676–1686 (2008).
24. Bünger, M. *et al.* Genome-wide analysis of PPARα activation in murine small intestine. *Physiol. Genomics* **30**, 192–204 (2007).
25. Simmen, F.A. *et al.* Dysregulation of intestinal crypt cell proliferation and villus cell migration in mice lacking Kruppel-like factor 9. *Am. J. Physiol. Gastrointest. Liver Physiol.* **292**, G1757–G1769 (2007).
26. Falcon, A. *et al.* FATP2 is a hepatic fatty acid transporter and peroxisomal very long-chain acyl-CoA synthetase. *Am. J. Physiol. Endocrinol. Metab.* **299**, E384–E393 (2010).
27. Lehto, M. *et al.* The OSBP-related protein family in humans. *J. Lipid Res.* **42**, 1203–1213 (2001).

28. Hwang, B., Jeoung, N.H. & Harris, R.A. Pyruvate dehydrogenase kinase isoenzyme 4 (PDHK4) deficiency attenuates the long-term negative effects of a high-saturated fat diet. *Biochem. J.* **423**, 243–252 (2009).
29. Watschinger, K. *et al.* Identification of the gene encoding alkylglycerol monooxygenase defines a third class of tetrahydrobiopterin-dependent enzymes. *Proc. Natl. Acad. Sci. USA* **107**, 13672–13677 (2010).
30. Berger, K., Winzell, M.S., Mei, J. & Erlanson-Albertsson, C. Enterostatin and its target mechanisms during regulation of fat intake. *Physiol. Behav.* **83**, 623–630 (2004).
31. Ahima, R.S. & Flier, J.S. Leptin. *Annu. Rev. Physiol.* **62**, 413–437 (2000).
32. Skinner, J. *et al.* Construct and compare gene coexpression networks with DAPfinder and DAPview. *BMC Bioinformatics* **12**, 286 (2011).
33. Nishiyama, Y. *et al.* Homeostatic regulation of intestinal villous epithelia by B lymphocytes. *J. Immunol.* **168**, 2626–2633 (2002).
34. Degrandi, D. *et al.* Extensive characterization of IFN-induced GTPases mGBP1 to mGBP10 involved in host defense. *J. Immunol.* **179**, 7729–7740 (2007).
35. Yanai, H., Savitsky, D., Tamura, T. & Taniguchi, T. Regulation of the cytosolic DNA-sensing system in innate immunity: a current view. *Curr. Opin. Immunol.* **21**, 17–22 (2009).
36. Turnbaugh, P.J. & Gordon, J.I. The core gut microbiome, energy balance and obesity. *J. Physiol. (Lond.)* **587**, 4153–4158 (2009).
37. Hughes, W.S., Cerda, J.J., Holtzapple, P. & Brooks, F.P. Primary hypogammaglobulinemia and malabsorption. *Ann. Intern. Med.* **74**, 903–910 (1971).
38. Mannon, P.J. *et al.* Excess IL-12 but not IL-23 accompanies the inflammatory bowel disease associated with common variable immunodeficiency. *Gastroenterology* **131**, 748–756 (2006).
39. Agarwal, S. & Mayer, L. Pathogenesis and treatment of gastrointestinal disease in antibody deficiency syndromes. *J. Allergy Clin. Immunol.* **124**, 658–664 (2009).
40. Koch, J. *et al.* Steatorrhea: a common manifestation in patients with HIV/AIDS. *Nutrition* **12**, 507–510 (1996).
41. Ullrich, R., Riecken, E.O. & Zeitz, M. Human immunodeficiency virus–induced enteropathy. *Immunol. Res.* **10**, 456–464 (1991).
42. Sanford, J.P., Favour, C.B. & Tribeman, MS. Absence of serum gamma globulins in an adult. *N. Engl. J. Med.* **250**, 1027–1029 (1954).
43. Owens, S.R. & Greenson, J.K. The pathology of malabsorption: current concepts. *Histopathology* **50**, 64–82 (2007).
44. Malamut, G. *et al.* The enteropathy associated with common variable immunodeficiency: the delineated frontiers with celiac disease. *Am. J. Gastroenterol.* **105**, 2262–2275 (2010).
45. Lerner, P. *et al.* The gut mucosal viral reservoir in HIV-infected patients is not the major source of rebound plasma viremia following interruption of highly active antiretroviral therapy. *J. Virol.* **85**, 4772–4782 (2011).
46. Crawford, A., Macleod, M., Schumacher, T., Corlett, L. & Gray, D. Primary T cell expansion and differentiation *in vivo* requires antigen presentation by B cells. *J. Immunol.* **176**, 3498–3506 (2006).
47. Wojciechowski, W. *et al.* Cytokine-producing effector B cells regulate type 2 immunity to *H. polygyrus*. *Immunity* **30**, 421–433 (2009).
48. Cong, Y., Feng, T., Fujihashi, K., Schoeb, T.R. & Elson, C.O. A dominant, coordinated T regulatory cell–IgA response to the intestinal microbiota. *Proc. Natl. Acad. Sci. USA* **106**, 19256–19261 (2009).
49. Peterson, D.A., McNulty, N.P., Guruge, J.L. & Gordon, J.I. IgA response to symbiotic bacteria as a mediator of gut homeostasis. *Cell Host Microbe* **2**, 328–339 (2007).
50. Obata, T. *et al.* Indigenous opportunistic bacteria inhabit mammalian gut-associated lymphoid tissues and share a mucosal antibody-mediated symbiosis. *Proc. Natl. Acad. Sci. USA* **107**, 7419–7424 (2010).
51. Scamurra, R.W. *et al.* Mucosal plasma cell repertoire during HIV-1 infection. *J. Immunol.* **169**, 4008–4016 (2002).
52. Kotler, D.P., Scholes, J.V. & Tierney, A.R. Intestinal plasma cell alterations in acquired immunodeficiency syndrome. *Dig. Dis. Sci.* **32**, 129–138 (1987).

ONLINE METHODS

Mice. B10.A, B10.A-μMT, BALB/c, BALB/c-JhKO and B10.A-RagKO mice were obtained from the NIAID contract facility at Taconic or Taconic Farms. The knockout mice had no detectable IgA levels[53]. Antibody-deficient activation-induced cytidine deaminase /μS and IgA KO mice were provided by T.D. Randall and S. Epstein, respectively. Germ-free B10.A-μMT and controls were re-derived and maintained at Taconic farms Gnotobiotic Center. C57BL/6-JhKO and control germ-free mice were maintained at McMaster University and at the National Gnotobiotic Rodent Resource Center at the University of North Carolina. Mice used in the experiments were of both genders and 2–6 months old. The study was approved by the NIH Animal Care and Use Committee. Mouse small intestines were snap frozen and processed as described in the **Supplementary Methods**.

Human samples. Duodenal biopsies were obtained from three individuals with CVID with gastrointestinal syndrome and from three immunodeficient individuals without this syndrome used as controls. The CVID biopsies showed shortening of villi and lymphocyte infiltrations, whereas control biopsies were normal. The samples were snap frozen on dry ice and kept at −80 °C until RNA isolation. The procedures were approved by the Institutional Review Boards of NIAID and Mount Sinai Medical Center with informed consent obtained from the subjects.

Microarray sample preparation and hybridization. RNA samples were isolated, labeled and hybridized, and arrays were scanned as described in the **Supplementary Methods**.

Analysis of microarray data. All microarray data that passed quality control were analyzed using BRB Array Tools developed by the Biometric Research Branch of the National Cancer Institute under the direction of R. Simon (http://linus.nci.nih.gov/BRB-ArrayTools.html). Array data were filtered to limit analysis to probes with greater than 50% of samples showing spot intensities of >10 and spot sizes >10 pixels, and a median normalization was applied.

Differentially expressed genes between groups of samples were identified by random variance *t* test with adjustment for multiple hypotheses by setting the false discovery rate (FDR) below 10% in BRB Array Tools. In particular, for discovery of B-cell KO profile (**Fig. 1a**), gene expression was first compared in μMT versus heterozygous littermate controls ($n = 12$ per group). Using intentionally relaxed criteria of $P < 0.05$, ~700 differentially expressed gene probes were found. As genes expressed by B lymphocytes would be likely to make up a proportion of downregulated genes, we performed microarrays on 15 samples of B lymphocytes to identify B cell–specific genes. We found 229 gene probes with higher expression in B lymphocytes than in BcKO intestines (FDR <10%), and excluded them from the profile. To identify the most robust fraction of the profile, we then validated the differences on 15 pairs of two types of BcKOs (B10.A-μMT and BALB/c-JhKO) and their respective WT nonlittermate control mice.

Summary metrics for **Figure 3d** were calculated by first normalizing each gene's value by dividing it by the median value for that gene in all mice. Then, for each mouse, separate median values for up-and downregulated genes of the profile were calculated, obtaining two values for each mouse.

For the analysis of Ppara and Klf9 knockout mice and humans with HIV, we used publicly available data from GEO (GDS2886, GDS2703 and GSE28177, respectively), which we imported and analyzed in BRB Array Tools. Functional enrichment analysis of the gene lists was performed to find Gene Ontology categories (biological process) statistically significantly overrepresented in the lists of interest comparing to the whole genome using ExPlain software (BIOBASE). Those categories with *P* values below 0.01, adjusted for multiple comparisons, were accepted. We used the TRANSFAC database within the ExPlain software (BIOBASE) to analyze transcription factor binding motifs and calculate enrichment for transcription factors in the gene list of interest compared to all promoters in the database or to a subset of 1,000 gene promoters that were expressed in jejunum and showed low variance across BcKO and control mice.

For correlation with human data, we obtained 219 human homologs among 280 differentially expressed genes in BcKO mice using the Mouse Genome Informatics website (http://www.informatics.jax.org/), and their gene expression was compared between human subjects with and without disease.

Reconstruction and analysis of the network. Using gene expression data from three independent groups of control mice (two groups of B10.A mice $n = 12$ and 17, one group of BALB/c mice $n = 10$), we performed a correlation analysis with the DAPfinder plug-in for BRB-ArrayTools[32]. We used this plug-in to calculate Pearson's correlation between all gene pairs of the BcKO profile. After calculation of correlations in each group independently, the results were combined, and only gene pairs present in all three data sets and with the same direction of correlation (positive or negative) were selected. We applied Fisher's inverse χ^2 method and selected gene pairs that had FDR-adjusted *P* value below 0.05. As expected for nonrandom biological networks, the distribution of nodes and connections follows power-law (*R*-squared = 0.852). The network was visualized in Cytoscape Software 2.6.3 (ref. 54). We used the MCODE v1.2 (Molecular Complex Detection)[55] plug-in for Cytoscape to identify clusters (subnetworks) of correlated genes. We searched for subnetworks/clusters that had a K score above three, using the node score cut-off of 0.35. The two top ranked subnetworks were selected for further analyses, as all other subnetworks were representing parts of the first two.

Analysis of jejunal microbiota. DNA from jejunum content was isolated using QIAamp DNA Stool Mini Kit (Qiagen) following the protocol with optional 10-min 90 °C incubation for better lysis of bacteria. Ten nanograms of DNA were amplified using QuantiFast SYBR Green PCR Mix (Qiagen) and universal bacterial primers[56] for quantification of total bacterial DNA.

We used 454 pyrosequencing of genes endcoding 16S rRNA genes to characterize jejunal microbiome (see details in **Supplementary Methods**). Each processed 16S rRNA gene sequence was classified using the RDP Naive Bayesian Classifier[57] with a confidence level cutoff of 0.5. Sequences were also clustered into operation taxonomic units using Mothur v. 1.10 (ref. 58).

Metabolic measurements. Metabolic measurements are described in the **Supplementary Methods**.

***In vitro* assay.** MODE-K cells were incubated 3×10^5 per well in a 12-well plate in 1 ml of DMEM (Invitrogen) supplemented with 10% FBS (Gibco) with 5 μM CpG ODN 1585 (Invivogen); 1×10^7 per ml heat-treated *E. coli* (Invitrogen); IFN (IFN-α 500 U ml^{-1} and IFN-γ 100 U ml^{-1}; PBL InterferonSource); 1 μg ml^{-1} LPS (Sigma) or 10 μg ml^{-1} poly I:C (Invitrogen) for 24 h.

Statistical analysis of data (except for microarrays). For paired comparisons we used paired *t* test or Wilcoxon matched-paired signed-ranked test. For nonpaired comparisons we used *t* test or Mann-Whitney test. We used nonparametric tests in case the data does not pass normality test ($P < 0.05$). The outliers were identified as values outside of mean ± three s.d. and removed from the further analysis.

Additional methods. Detailed methodology is described in the **Supplementary Methods**.

53. Shulzhenko, N., Morgun, A. & Matzinger, P. Spontaneous mutation in the Cd79b gene leads to a block in B-lymphocyte development at the C (early pre-B) stage. *Genes Immun.* **10**, 722–726 (2009).
54. Cline, M.S. *et al.* Integration of biological networks and gene expression data using Cytoscape. *Nat. Protoc.* **2**, 2366–2382 (2007).
55. Bader, G.D. & Hogue, C.W. An automated method for finding molecular complexes in large protein interaction networks. *BMC Bioinformatics* **4**, 2 (2003).
56. Barman, M. *et al.* Enteric salmonellosis disrupts the microbial ecology of the murine gastrointestinal tract. *Infect. Immun.* **76**, 907–915 (2008).
57. Cole, J.R. *et al.* The Ribosomal Database Project (RDP-II): previewing a new autoaligner that allows regular updates and the new prokaryotic taxonomy. *Nucleic Acids Res.* **31**, 442–443 (2003).
58. Schloss, P.D. *et al.* Introducing mothur: open-source, platform-independent, community-supported software for describing and comparing microbial communities. *Appl. Environ. Microbiol.* **75**, 7537–7541 (2009).

doi:10.1038/nm.2505